ARTICLE

Unraveling Ethylene Carbonate-Propylene Carbonate Disparity at Electrode Interface Using Femtosecond Sum Frequency Generation Vibrational Spectroscopy†

Zhuo Wang, Xiaoxuan Zheng, Zijian Ni, Shuji Ye*

Hefei National Research Center for Physical Sciences at the Microscale, Department of Chemical Physics, University of Science and Technology of China, Hefei 230026, China

(Dated: Received on August 2, 2024; Accepted on October 8, 2024)

Ethylene carbonate (EC) is an important electrolyte used in lithium-ion batteries due to its excellent electrochemical performance. However, propylene carbonate (PC) differs from EC by only one methyl substituent and exhibits markedly poor properties. The EC-PC disparity is still poorly understood at the molecular level. In this study, we demonstrated that femtosecond broadband sum frequency generation vibrational spectroscopy (SFG-VS) with simultaneous measurement of multiple polarization combinations provides a powerful probe for investigating the physicochemical processes at the electrode-electrolyte interface during the charge-discharge cycles of lithium batteries. Using monolayer graphene as the working electrode, we observed the distinct reaction outcomes of EC and PC on the electrode surface. The interfacial reaction of EC occurred only in the first charge-discharge cycle, while the interfacial reaction of PC was ongoing along with the charge-discharge cycles, which explains why EC is a better electrolyte choice than PC. This study provides direct experimental evidence in elucidating the differences in interfacial performance between EC and PC, facilitating a deeper understanding of battery interface reactions and guiding the design of high-performance lithium-ion batteries.

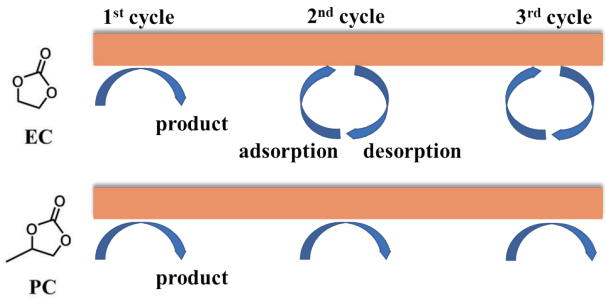

Key words: Sum frequency generation vibrational spectroscopy, Ethylene carbonate, Propylene carbonate, Solid electrolyte interphase

I. INTRODUCTION

Insight into the dynamic behavior of electrolytes at electrode surface is critical for understanding the structure-property relationship of different electrolytes and designing lithium-ion batteries (LIBs) with excellent performance and high safety [1–7]. Among the electrolytes, ethylene carbonate (EC) and propylene carbonate (PC) are the most popular electrolytes of LIBs [8, 9]. Despite their similar structures and chemical properties, EC-based electrolytes have been used as a benchmark electrolyte in industry due to its excellent electrochemical performance since the commercial inception of LIBs in the 1990s. However, PC, differing from EC by only one methyl substituent, exhibits markedly different interfacial properties and has limited commercial application [8, 10–12]. The tiny structural difference due to a single methyl group between EC and PC surprisingly causes large differences in reactivity and degradation products of these solvents. This

† Part of Special Issue "In Memory of Prof. Xingxiao Ma on the occasion of his 90th Anniversary".

* Author to whom correspondence should be addressed. E-mail: shujiye@ustc.edu.cn

EC-PC disparity has puzzled electrochemists for decades [8, 10–12].

Several prevailing hypotheses have been proposed to elucidate the differences in interfacial performance between EC and PC. Auerbach's group suggested that the fundamental pathways of interfacial reduction for EC and PC are analogous, and the pronounced differences in their interfacial properties stem from the distinct physicochemical properties of their respective reduction products [13]. The reduction of PC is thought to yield 1,2-propylene dicarbonate (LPDC), which forms a loosely packed, chain-like structure with poor cohesive strength and resistance to dissolution, impeding the formation of a stable solid electrolyte interphase (SEI) [1–7]. Conversely, the reduction of EC is known to produce ethylene dicarbonate, which, due to the absence of a methyl group, adopts a more planar conformation that readily condenses into a compact film on the electrode surface. Zhuang and colleagues offered an alternative perspective, suggesting that the differences between EC and PC stem from their distinct interfacial reaction pathways [14]. Based on Fourier-transform infrared spectroscopy data which indicate co-intercalation of PC with Li^+ into graphite interlayers, they propose that PC may undergo a two-electron reduction pathway, diverging from the one-electron pathway of EC. The reduction products of PC are suggested to be Li_2CO_3 and organic gases, rather than LPDC, which do not contribute to the formation of a protective interface. Li and co-workers attributed the interfacial performance differences to the differential solvation capabilities of EC and PC for Li^+ ions [10]. The competitive solvation of Li^+ by anions and solvent molecules determines the composition of the Li^+ solvation complex, and the subsequent de-solvation process during Li^+ precipitation dictates the initial composition of the interfacial reaction. PC molecules exhibit a stronger binding affinity for Li^+ compared to the anion (PF_6^-), leading to a predominance of LPDC at the interface. In contrast, EC molecules exhibit weaker binding affinity for Li^+, resulting in the presence of anionic reduction products such as LiF, which are conducive to the formation of a dense and stable interface.

Despite numerous explanations for the interfacial performance differences between EC and PC have been proposed [11, 12], most are derived from indirect evidence or theoretical calculations. There remains a significant gap in direct experimental validation of these hypotheses. Since the concept of the SEI was introduced, its intricate bilayer structure and dynamic equilibrium have posed challenges for real-time, *in situ* investigation [2, 15–23]. In this work, we demonstrated that simultaneous measurement of multiple polarization combinations using femtosecond broadband sum frequency generation vibrational spectroscopy (SFG-VS) provided a powerful tool for real-time and *in situ* monitoring of the electrode-electrolyte interface during charge-discharge cycles. SFG is a second-order nonlinear optical technology that has unique surface and interface selectivity, immune to water signals, and can offer information in real time, *in situ* without any exogenous labeling [24–27]. SFG has emerged as a powerful tool for studying molecular structure and dynamics at interfaces including electrode/electrolyte interface [7, 28]. In principle, the single polarization SFG system can only obtain single-polarization-combination information in one experiment and therefore is difficult to discern the contribution of interfacial molecular number and orientation of the probed chemical groups to the changes in the sum frequency signal. For a complex system such as battery interfacial reactions, traditional single-polarization SFG techniques no longer suffice to meet the demands of experimental research. In contrast, multiple polarization SFG, capable of acquiring information from multiple polarizations simultaneously, greatly facilitates the characterization of interfacial molecular structures and enables precise measurement of the interfacial reactions. By comparing the behavior of PC and EC molecules at the graphene electrode, we dissected the impact of electrolyte solution molecules on interfacial reactions and deduced the pathways involved. It is found that EC interfacial reactions are primarily confined to the first charge-discharge cycle, with subsequent cycles showing only molecular adsorption and desorption. In contrast, PC electrolytes exhibit a persistent physicochemical process that endures across multiple cycles, accompanied by continuous PC molecule consumption. The relative instability of PC at the interface is deleterious to the battery system's application. The direct experimental evidence garnered from SFG spectroscopy measurements offers deep insights into the molecular-level differences between EC and PC at the electrode surface.

II. EXPERIMENTS

A. Materials and sample preparation

Diethyl carbonate (DEC, with a purity > 99.99%),

DOI: 10.1063/1674-0068/cjcp2408102

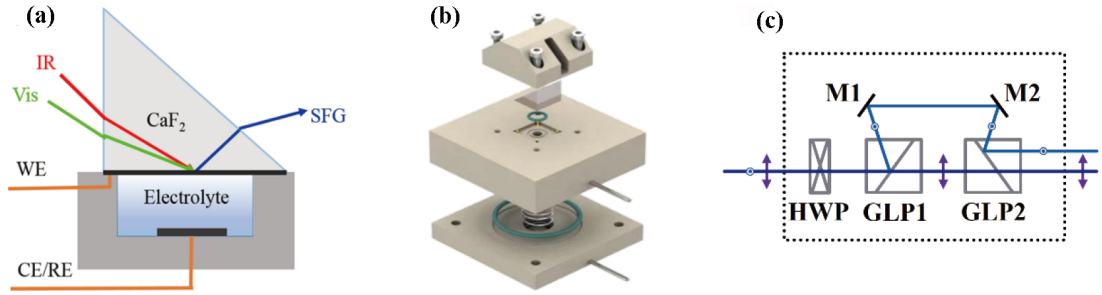

FIG. 1 Schematic diagram (a) and actual setup (b) of the SFG-electrochemical measurement system. (c) Schematic diagrams of multi-polarization combination separation module. WE=working electrode, CE=counter electrode, RE=reference electrode, GLP=glan-laser polarizer, M= mirror, and HWP=half-wave plate.

ethylene carbonate (EC, with a purity>98%), and propylene carbonate (PC, with a purity>99%) were purchased from Aladdin. All the chemicals were used as received. The monolayer graphene was purchased from Shenzhen Six Carbon Technology Co., Ltd. and was artificially transferred to the CaF_2 prismatic substrate as the working electrode. Lithium metal flakes were purchased from Xinghua Benote Battery Materials Co., Ltd. as counter and reference electrodes, and both were assembled with the electrolyte solution in an argon glove box to form a model battery, which was left to stand for 2 h after the battery system was assembled before measurement, as shown in FIG. 1.

B. Multiple-polarized SFG-VS experiments

Simultaneous measurement of multiple polarization combinations was performed using a multi-polarization signal acquisition module previously developed in our laboratory [28–30]. The schematic is shown in FIG. 1(c). In the multi-polarization-combination module, two Glan-laser polarizers (GLPs) were used to separate the p and s components. The p-polarized beam was continued to pass through the first (GLP1) and the second (GLP2) while the s-polarized beam was reflected by GLP1, mirrors (M1 and M2) and GLP2. After multiple reflection of s-polarized beam, a 2.6 mm vertical displacement between p- and s- polarized beam was generated [24–26]. Consequently, simultaneous measurement of multiple polarization combinations (*e.g.*, ppp polarization and ssp polarization) was conducted by imaging at different vertical pixel array on the ICCD camera. The improvement in experiments will aid in the characterization of interfacial molecular structure and the precise measurement of interfacial reactions. In this study, all the ssp and ppp SFG spectra were acquired by the multi-polarization-combination module. The SFG spectra were normalized by the energy profiles of the IR pulses which were determined by the SFG signals from the gold layer coated at the CaF_2 prism.

C. Electrochemical measurements

Electrochemical measurements were performed using a CHI660e workstation, which was purchased from Shanghai Chenhua Instrument Co., Ltd. The charging and discharging operation of the battery in this study was performed by cyclic voltammetry (CV), with graphene as the working electrode and lithium metal as the counter/reference electrode. The charging and discharging potential were 3 V−0.005 V−3 V with a charging and discharging rate of 0.001 V/s. The cycle period was 3 cycles.

III. RESULTS AND DISCUSSION

We first investigated the adsorption behavior of electrolytes on the surface of graphene electrodes. FIG. 2 illustrates the comparative steady-state adsorption SFG spectra of the graphene electrode interface with mixed DEC/EC and DEC/PC solutions against those of pristine DEC, EC, and PC. A discernible feature in the SFG spectra for DEC molecules is the manifestation of *cis*- and *trans*- isomers, with distinct C=O bond orientations correlating to frequencies of 1767 cm^{-1} (towards the electrode) and 1745 cm^{-1} (towards the electrolyte solution) [7, 31, 32]. The SFG signals for EC were primarily observed at 1767 cm^{-1} (Fermi resonance), 1780 cm^{-1} (C=O stretching vibration, oriented away from the bulk phase), and 1790 cm^{-1} (C=O stretching vibration, oriented towards the electrode interface), with two broad peaks at 1837 cm^{-1} and 1867 cm^{-1} (C=O symmetric and antisymmetric stretching vibration) [7, 33–36]. The signal intensities for these

DOI: 10.1063/1674-0068/cjcp2408102

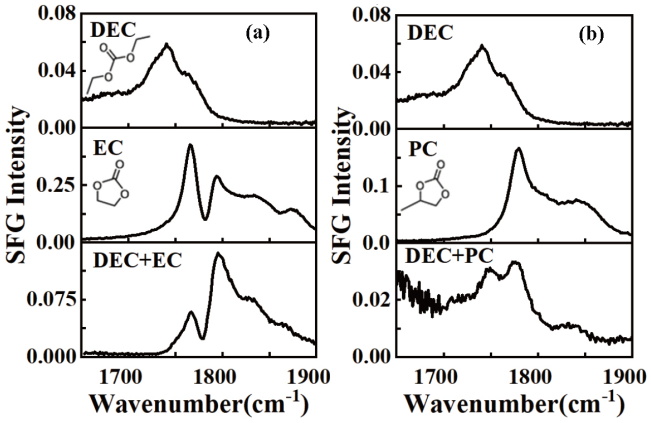

FIG. 2 (a) Steady-state ppp spectra of DEC, EC, and mixed electrolyte solution EC/DEC in the region of 1650 – 1900 cm^{-1} on the surface of graphene electrode. (b) Steady-state ppp spectra of DEC, PC, and mixed electrolyte solution PC/DEC in the region of 1650–1900 cm^{-1} on the surface of graphene electrode.

peaks differed by nearly an order of magnitude, indicating a significant disparity in the effective second-order hyperpolarizability rates between the two molecular species. As shown in FIG. 2(a), in the case of the mixed DEC/EC solution, prior to battery conduction, the SFG spectra can be considered as a composite of the pure DEC and EC spectra. Two strong signals were observed at 1767 cm^{-1} and 1790 cm^{-1}, with a reduced intensity ratio compared to that of pure EC. This reduction is attributed to the overlapping signals of DEC and EC at 1767 cm^{-1}, which are out of phase and thus cancel each other out, leading to an overall diminished signal intensity. The signal at 1790 cm^{-1} is exclusive to EC, arising from the C=O stretching oriented towards the electrode interface. A faint signal at 1780 cm^{-1} corresponds to the C=O group of EC oriented away from the electrode, while broad peaks of EC are present at 1837 cm^{-1} and 1867 cm^{-1}. A discreet signal at approximately 1749 cm^{-1} is indicative of the DEC-specific C=O stretching mode. The observations indicate that for an electrolyte solution of EC/DEC (1:1 volumetric ratio), there is adsorption of both types of molecules at the electrode surface, with EC signals being more pronounced due to the difference in effective second-order hyperpolarizability rates. The middle panel in FIG. 2(b) delineates the SFG signals for PC, with a principal peak at 1778 cm^{-1} and a faint broad peak at higher wavenumbers (1832 cm^{-1}). For the DEC/PC mixed solution, distinct signals for DEC (1749 cm^{-1}) and PC (1778 cm^{-1}) are evident [37, 38], with an overall decrease in signal intensity compared to the pure solutions.

After that, we compared the differences between the EC and PC interfaces with charging and discharging conditions. For the EC interface, the cyclic voltammetry curve (FIG. 3(a)) during the first charge-discharge cycle shows a distinct reaction process around 1.5 V, which diminishes in subsequent cycles. FIG. 3 (b) and (c) present the complete ppp and ssp SFG spectra of the electrode surface as a function of electrode potential. It is evident that as the charge-discharge process progresses with an electrolyte solution of EC/DEC (1:1), there is a noticeable trend of change in the SFG spectra, indicative of alterations in the physicochemical behavior of adsorbed molecules at the electrode surface in response to potential changes. The variations in SFG signal intensity can be attributed to three factors: changes in molecular orientation at the interface, which are discernible from the combined trends of ppp and ssp SFG spectra; alterations in the number of molecules adsorbed due to changes in interfacial electrode potential; and changes in the number of molecules due to interfacial reactions, which can be inferred from the reversibility of the signals post one charge-discharge cycle. Detailed analysis of the spectra during the first charge-discharge cycle (FIG. S2 in Supplementary materials, SM) reveals that the SFG signal changes are bifurcated into two parts: the first stage from 2 V to 1.5 V, where a distinct reaction process is observed in the CV curve, corresponding to the reaction phase of EC molecules, leading to a decrease in SFG signal due to reduced molecular adsorption. The second stage spans from 1.5 V to 0.005 V to 3 V, representing an adsorption-desorption process of interfacial molecules, with periodic changes in SFG signal intensity that exhibit a temporal lag relative to the potential changes. FIG. S3 (a) and (b) in SM display the SFG spectra at various potential points during the second and third cycles. FIG. S3 (c) and (d) in SM depict the trends in peak intensity variation with electrode potential. Compared with the first cycle, a slight decrease in SFG signal intensity around 1.5 V during the second cycle indicates a residual EC reduction reaction, which disappears during the third cycle, leaving only a pronounced periodic variation in SFG signal intensity with potential, attributed to the adsorption-desorption of molecules near the electrode due to changes in the electric double layer. Furthermore, the spectra reveal that at low adsorption sites (3 V), the SFG signal decrease is accompanied by a pronounced

DOI: 10.1063/1674-0068/cjcp2408102

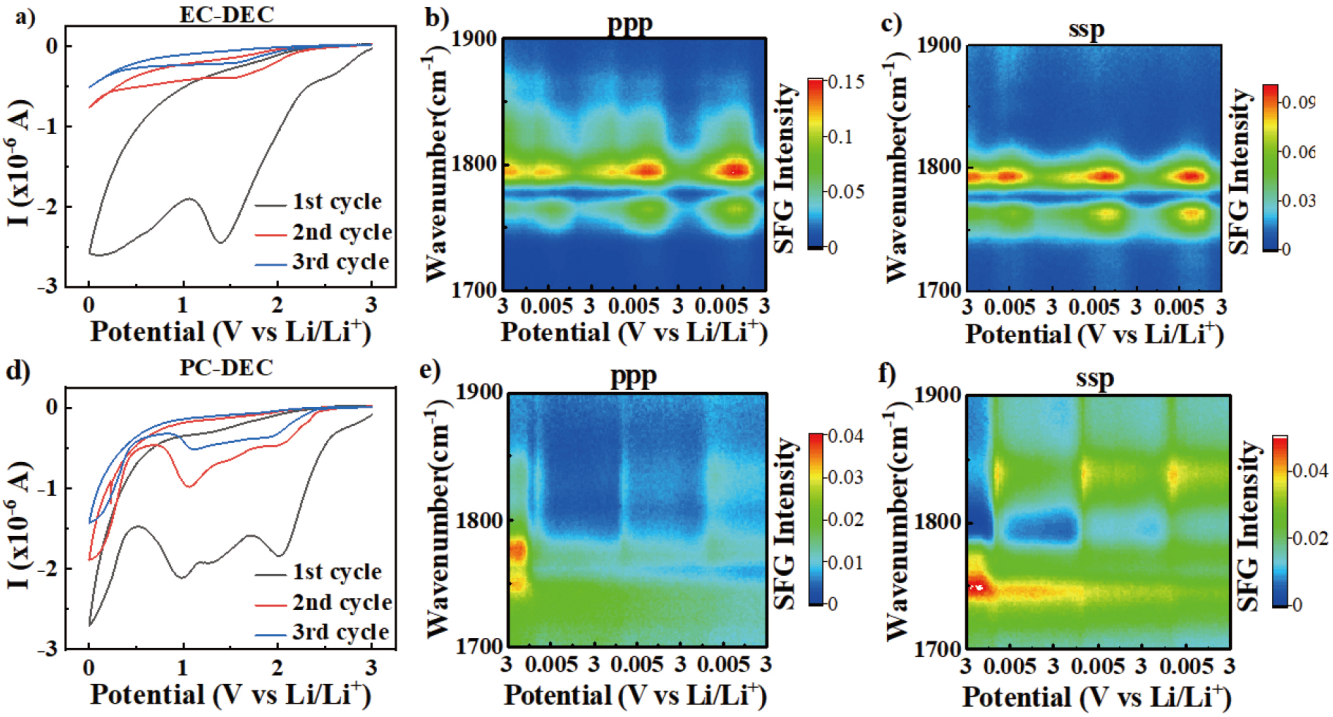

FIG. 3 Upper panel: battery system with EC/DEC as electrolyte solution at applied cyclic potential. (a) Cyclic voltammetry curves during charging and discharging of the battery; complete spectrum of SFG signal evolution with electrode potential in the 1700–1900 cm^{-1} region at the graphene electrode surface of (b) ppp polarization and (c) ssp polarization. Lower panel: battery system with PC/DEC as electrolyte solution at applied cyclic potential. (d) cyclic voltammetry curves during charging and discharging of the battery; complete spectrum of SFG signal evolution with electrode potential in the 1700–1900 cm^{-1} region at the graphene electrode surface of (e) ppp polarization and (f) ssp polarization.

DEC signal (1749 cm^{-1}). This phenomenon is related to the dielectric properties of the various molecules in solution, with EC exhibiting a higher relative permittivity (89.78) compared with DEC (2.81) [39]. A higher permittivity corresponds to greater sensitivity to potential changes, leading to more pronounced adsorption-desorption behavior for EC at the electrode surface. The complete change in peak signal intensity across three cycles is presented in FIG. 4(a) and (b). Previous theoretical calculations suggested that the decomposition of EC molecules involves ring-opening reactions, yielding long-chain carbonate esters. Isolated EC molecules possess relatively high redox potentials [40–43], making them relatively stable at the interface and resistant to reaction, which aligns with experimental findings that show a clear adsorption-desorption process of EC molecules on the interface without observable reduction during the second and third cycles.

For the PC interface, the CV curve (FIG. 3(d)) during charge-discharge cycles reveals distinct reaction processes around 2 V and 0.9 V during the first cycle. The reaction at 2 V diminishes in the second and third cycles, while that at 0.9 V weakens but persists. FIG. 3 (e) and (f) present the complete ppp and ssp SFG spectra of the electrode interface as a function of electrode potential, showing a clear trend of periodic variation with potential changes for an electrolyte solution of PC/DEC (1:1). Detailed analysis of the first charge-discharge cycle (FIG. S4 in SM) indicates that the SFG spectra changes are divided into two parts: the first part, from 2 V to 1.2 V, corresponds to the initial reaction phase of the electrolyte solvent molecules, leading to a decrease in signal intensity. The second part, from 1.2 V to 0.9 V, represents a subsequent reaction process of PC molecules, with a specific potential point (~0.9 V) where PC molecules undergo further reactions, resulting in a characteristic rise and fall in SFG signal. The second cycle (FIG. S5(a, b) in SM) shows no emergence of new signals, with the second and third cycles exhibiting a similar trend in peak signal intensity variation (FIG. S5(c) in SM). Specifically, from 3 V to 1.5 V, the SFG signal peak intensities remain relatively unchanged, indicating interface stability. From 1.5 V to 0.9 V to 0.005 V, the signal intensities for PC molecules (1777 cm^{-1} and 1832 cm^{-1}) exhibit a rise and fall, while the DEC signal (1749 cm^{-1}) slightly decreases. Post

DOI: 10.1063/1674-0068/cjcp2408102

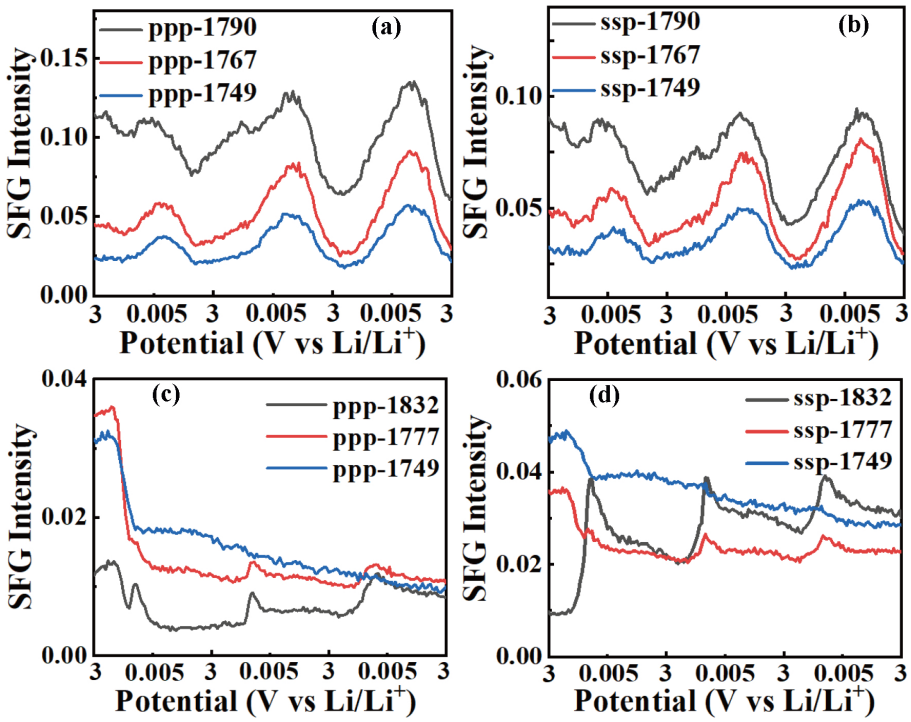

FIG. 4 Upper panel: complete spectra of the evolution of the signal intensity of the three periodic peaks as a function of the electrode potential for EC. Image of the SFG spectra under (a) ppp polarization and (b) ssp polarization of the signal intensity of the three peaks 1790 cm^{-1} (black line), 1767 cm^{-1} (red line), 1749 cm^{-1} (blue line) as a function of the electrode potential. Lower panel: complete spectra of the evolution of the signal intensity of the three periodic peaks as a function of the electrode potential for PC. Images of the SFG spectra under (c) ppp polarization and (d) ssp polarization with the signal intensity of the three peaks 1832 cm^{-1} (black line), 1777 cm^{-1} (red line), 1749 cm^{-1} (blue line) as a function of the electrode potential.

0.005 V to 3 V, the signal intensities remain largely unchanged. In conclusion, our findings reveal that EC molecules exhibit low reactivity, with the initial cycle of electrode interfacial reactions forming a protective layer that prevents further reaction progression, leaving only solvent molecule adsorption and desorption. In contrast, PC molecules, after reacting in the first cycle, continue to interact with interfacial products, leading to ongoing electrolyte solution consumption, which significantly impacts its practical application. Meanwhile, in the presence of PC, the continuous interfacial reaction of DEC molecules at the electrode interface reduces the reversibility of the electrode during charge-discharge cycles, which further explains why EC is a better electrolyte choice than PC. The assignment of the high-wavenumber signal peak is multifaceted [44]. On one hand, quantum chemical calculations indicate a propensity for PC molecules to form aggregates, which can induce a shift in the carbonyl (C=O) vibrational peak positions. This phenomenon accounts for the faint high-wavenumber signals observed in the steady-state ppp polarization SFG spectra prior to electrification. On the other hand, the PC molecule, undergoing distinct ring-opening reactions at various reactive sites to yield intermediate products (such as formation of $\cdot COOCH_2CH(CH_3)O\cdot$ at the C=O group linkage with the ring oxygen, and $\cdot OCOOCH_2CH(CH_3)\cdot$ at the ring oxygen and CH group linkage), may further react to form oxycarbonates ($(R_1OOC)O(COOR_2)$). Extant research has demonstrated that the C=O stretching vibrational signals of oxycarbonates exhibit a high-wavenumber shift of several tens of wavenumbers relative to those of carbonates (*e.g.*, the C=O signals for oxycarbonates like diethyl oxalate are found at 1823 cm^{-1} and 1781 cm^{-1} in IR spectroscopy, contrasting with the 1747 cm^{-1} signal for the carbonate diethyl carbonate, data derived from chemical databases). Accordingly, we attribute the emergence of new signal peaks during the battery charge-discharge cycles to the formation of oxycarbonate species. Our findings elucidate a two-step interfacial reaction mechanism for PC molecules. The initial reaction predominantly occurs within the 2 V to 1.2 V range during the first cycle, where PC molecules decompose to form an interfacial

DOI: 10.1063/1674-0068/cjcp2408102

barrier. This process is analogous to the decomposition of EC molecules, and its outcome prevents the recurrence of this reaction in subsequent cycles. The second reaction step transpires at approximately 0.9 V, where PC molecules undergo ring-opening via various pathways at this potential, generating new free radical intermediates that react with the products of the first reaction to yield oxycarbonate compounds. These oxycarbonates are inherently unstable and prone to decomposition, which is manifested in the spectral profile as a recurring pattern of signal increase followed by decrease at specific potential points across three cycles. Additionally, a continuous decline in the DEC molecule signal is observed in the second and third cycles, indicative of the PC reaction products displacing DEC molecules at the electrode, thereby diminishing its signal.

In summary, EC molecules exhibit low reactivity, with the interfacial reactions of the first cycle culminating in a protective layer that inhibits further reaction progression, leaving only the adsorption and desorption of electrolyte solvent molecules. Specifically, during the first cycle, when the electrode potential is in the 2 V to 1.5 V range, EC molecules react at the interface. The products of EC reduction form a protective layer that prevents further reaction. Post the first cycle, only adsorption-desorption phenomena due to potential changes are observed. As the potential decreases, molecular adsorption intensifies, and as it increases, adsorption diminishes. The adsorption-desorption process exhibits a lag relative to potential changes, leading to a delayed response in peak signal intensity variations. In contrast, PC molecules exhibit high reactivity and instability during charging-discharging circles. Following the initial reaction cycle of PC molecules at the electrode, free PC molecules in the solution continue to react with interfacial products, leading to ongoing consumption of the electrolyte solution. This continuous consumption significantly impacts the practical application of PC-based electrolytes in battery systems.

IV. CONCLUSION

In this study, we have employed SFG-VS to measure the physicochemical transformations of electrolyte solvent molecules at the battery electrode interface during charge-discharge cycles. A comparative analysis was conducted to elucidate the distinct impacts of EC and PC on the interfacial reactions of the electrode. Our findings have delineated the divergent pathways of PC and EC at the electrode interface. The interfacial reactions involving EC are predominantly confined to the initial charge-discharge cycle, with subsequent cycles revealing only the adsorption and desorption of molecules at the interface. In contrast, the PC electrolyte exhibits a persistent physicochemical process that endures across multiple charge-discharge cycles, characterized by the continuous consumption of PC molecules. The comparative instability of PC at the interface is detrimental to its application within battery systems. The insights gleaned from this research are of paramount importance for advancing our understanding of the formation of the SEI and for the enhancement of lithium-ion battery performance. By distinguishing the roles of EC and PC at the electrode interface, this study contributes to the development of strategies for optimizing electrolyte formulations and, by extension, the overall efficiency and longevity of lithium-ion batteries. In addition, our work also highlights the power of the SFG-VS technique in revealing the dynamic processes occurring at the electrode-electrolyte interfaces, which is essential for the rational design and optimization of electrolyte formulations to enhance battery performance.

Supplementary materials: Detailed SFG spectra of the electrode surface during the first, second, and third cycles with electrolyte EC/DEC and PC/DEC are shown.

V. NOTES

The authors declare no competing financial interest.

VI. ACKNOWLEDGMENTS

This work was supported by the National Natural Science Foundation of China (No.21925302), and the Strategic Priority Research Program of the Chinese Academy of Sciences (XDB0450202).

[1] M. Gauthier, T. J. Carney, A. Grimaud, L. Giordano, N. Pour, H. H. Chang, D. P. Fenning, S. F. Lux, O. Paschos, C. Bauer, F. Maglia, S. Lupart, P. Lamp, and Y. Shao-Horn, J. Phys. Chem. Lett. **6**, 4653 (2015).

DOI: 10.1063/1674-0068/cjcp2408102

[2] E. Peled, D. Golodnitsky, and G. Ardel, J. Electrochem. Soc. **144**, L208 (1997).
[3] D. Aurbach, B. Markovsky, M. D. Levi, E. Levi, A. Schechter, M. Moshkovich, and Y. Cohen, J. Power Sources **81/82**, 95 (1999).
[4] K. Edström, T. Gustafsson, and J. O. Thomas, Electrochim. Acta **50**, 397 (2004).
[5] D. Guyomard and J. M. Tarascon, J. Electrochem. Soc. **140**, 3071 (1993).
[6] K. Xu, Chem. Rev. **114**, 11503 (2014).
[7] Z. Wang, Q. B. Pei, M. M. Wang, J. J. Tan, and S. J. Ye, Langmuir **39**, 2015 (2023).
[8] K. Xu, J. Electrochem. Soc. **156**, A751 (2009).
[9] P. Ganesh, D. E Jiang, and P. R. C. Kent, J. Phys. Chem. B **115**, 3085 (2011).
[10] L. D. Xing, X. W. Zheng, M. Schroeder, J. Alvarado, A. von Wald Cresce, K. Xu, Q. S. Li, and W. S. Li, Acc. Chem. Res. **51**, 282 (2018).
[11] T. Melin, R. Lundström, and E. J. Berg, Adv. Mater. Interfaces **9**, 2101258 (2022).
[12] J. X. Zhang, J. W. Yang, L. M. Yang, H. Lu, H. Liu, and B. Zheng, Mater. Adv. **2**, 1747 (2021).
[13] D. Aurbach, H. Teller, and E. Levi, J. Electrochem. Soc. **149**, A1255 (2002).
[14] G. V. Zhuang, H. Yang, B. Blizanac, and P. N. Ross Jr., Electrochem. Solid-State Lett. **8**, A441 (2005).
[15] E. Peled, J. Electrochem. Soc. **126**, 2047 (1979).
[16] E. Peled, J. Power Sources **9**, 253 (1983).
[17] J. P. Gabano, *Lithium Batteries*, New York: Academic Press, (1983).
[18] K. Kanamura, H. Tamura, and Z. I. Takehara, J. Electroanal. Chem. **333**, 127 (1992).
[19] K. Kanamura, H. Tamura, S. Shiraishi, and Z. I. Takehara, J. Electrochem. Soc. **142**, 340 (1995).
[20] D. Aurbach, M. L. Daroux, P. W. Faguy, and E. Yeager, J. Electrochem. Soc. **134**, 1611 (1987).
[21] D. Aurbach, B. Markovsky, A. Shechter, Y. Ein-Eli, and H. Cohen, J. Electrochem. Soc. **143**, 3809 (1996).
[22] E. Peled, D. Golodnttsky, G. Ardel, C. Menachem, D. Bar Tow, and V. Eshkenazy, MRS Online Proc. Library **393**, 209 (1995).
[23] L. H. Zu, W. Zhang, L. B. Qu, L. L. Liu, W. Li, A. B. Yu, and D. Y. Zhao, Adv. Energy Mater. **10**, 2002152 (2020).
[24] Y. R. Shen, Nature **337**, 519 (1989).
[25] X. Zhuang, P. B. Miranda, D. Kim, and Y. R. Shen, Phys. Rev. B **59**, 12632 (1999).
[26] M. A. Belkin and Y. R. Shen, Int. Rev. Phys. Chem. **24**, 257 (2005).
[27] C. A. Rivera and J. T. Fourkas, Int. Rev. Phys. Chem. **30**, 409 (2011).
[28] Z. Wang, J. J. Tan, Z. Yang, Y. Luo, and S. J. Ye, J. Phys. Chem. Lett. **13**, 3224 (2022).
[29] J. J. Tan, Y. Luo, and S. J. Ye, Chin. J. Chem. Phys. **30**, 671 (2017).
[30] J. J. Tan, J. H. Zhang, Y. Luo, and S. J. Ye, J. Am. Chem. Soc. **141**, 1941 (2019).
[31] A. K. Das, B. N. Rajasekhar, and S. Krishnakumar, J. Quant. Spectrosc. Radiat. Transfer **217**, 53 (2018).
[32] C. C. Yu, S. Imoto, T. Seki, K. Y. Chiang, S. M. Sun, M. Bonn, and Y. Nagata, J. Chem. Phys. **156**, 094703 (2022).
[33] D. Aurbach, A. Zaban, A. Schechter, Y. Ein-Eli, E. Zinigrad, and B. Markovsky, J. Electrochem. Soc. **142**, 2873 (1995).
[34] L. Yu, H. J. Liu, Y. Wang, N. Kuwata, M. Osawa, J. Kawamura, and S. Ye, Angew. Chem. Int. Ed. **52**, 5753 (2013).
[35] Q. L. Peng, H. J. Liu, and S. Ye, J. Electroanal. Chem. **800**, 134 (2017).
[36] B. Klassen, R. Aroca, M. Nazri, and G. A. Nazri, J. Phys. Chem. B **102**, 4795 (1998).
[37] H. J. Liu, Y. J. Tong, N. Kuwata, M. Osawa, J. Kawamura, and S. Ye, J. Phys. Chem. C **113**, 20531 (2009).
[38] L. Wang, Q. L. Peng, S. Ye, and A. Morita, J. Phys. Chem. C **120**, 15185 (2016).
[39] K. Xu, Chem. Rev. **104**, 4303 (2004).
[40] J. M. Yu, P. B. Balbuena, J. Budzien, and K. Leung, J. Electrochem. Soc. **158**, A400 (2011).
[41] K. Leung and J. L. Budzien, Phys. Chem. Chem. Phys. **12**, 6583 (2010).
[42] Y. Okamoto, J. Electrochem. Soc. **160**, A404 (2013).
[43] K. Leung and C. M. Tenney, J. Phys. Chem. C **117**, 24224 (2013).
[44] A. Von Wald Cresce, O. Borodin, and K. Xu, J. Phys. Chem. C **116**, 26111 (2012).

DOI: 10.1063/1674-0068/cjcp2408102